Int. J. Multiphase Flow Vol. 17, No. 2, pp. 179–189, 1991
Printed in Great Britain.

0301-9322/91 $3.00 + 0.00

GAS ENTRAINMENT IN A LONG LIQUID SLUG ADVANCING IN A NEAR HORIZONTAL PIPE

O. J. NYDAL[1] and P. ANDREUSSI[2]

[1]Institute for Energy Technology, 2007 Kjeller, Norway

[2]Department of Chemical Engineering, University of Pisa, Via Diotisalvi 2, 56100 Pisa, Italy

(Received 27 December 1989; in revised form 9 October 1990)

Abstract—The aeration of a liquid body advancing over a slow moving liquid layer in a pipe has been experimentally investigated with a conductance method. The 50 mm i.d. pipe section was close to horizontal and the fluids were air and water at atmospheric conditions. It has been found that net gas entrainment only occurs when the relative velocity between the advancing front and the liquid layer is greater than a limiting value. The rate of gas entrainment is proportional to the relative velocity between the advancing slug and the liquid layer, and to the interfacial width of the layer. Measured pressure drops, film heights and gas volume fractions in the advancing slug agree well with available correlations or with similar measurements taken under conditions of fully developed slug flow.

Key Words: gas entrainment, bubble production, liquid aeration, void fraction, slug flow

1. INTRODUCTION

Multiphase flow may be described in terms of a number of elementary interactions between the phases. In the present work attention is focused on one of these phenomena, the aeration of a liquid body by an impinging liquid stream.

In closed conduit flow the study of aeration processes is motivated by a number of engineering applications. The aeration of a liquid stream can dramatically change the flow characteristics and may lead to unpleasant flow instabilities and level surges.

Aeration may also be promoted in cases where it gives desired benefits. Self-aeration processes may provide effective and inexpensive means to increase mass transfer or to remove trapped gas pockets.

Previous workers [among others, Kalinske & Robertson (1943) and Ahmed *et al.* (1985)] have analysed the impingement of a wall jet on a stationary liquid level. The case considered in this work represents the opposite situation: the aeration of a liquid body advancing over a slow-moving liquid layer in a pipe. The work is directly related to the analysis of transient flow conditions experienced in two-phase pipelines, such as pigging or start-up operations and the occurrence of large terrain induced slugs.

The phenomenon investigated is also one of the elementary interactions between the gas and liquid phases occurring in two-phase slug flow. A dynamic model of slug flow requires information on the aeration process in front of each slug formed in the pipe. These slugs experience fluctuating upstream and downstream conditions that will determine the gas entrainment and other slug characteristics, such as length, velocity and pressure. The gas entrainment may also cause a large liquid slug to break up into a train of smaller slugs.

Analysis of the aeration process in slug flow has recently led Andreussi & Bendiksen (1989) to a semiempirical correlation for the gas fraction in the slugs. The results obtained in the present investigation can be very useful for developing a better founded relation.

In the present work the aeration process in an advancing water front has been analysed in a 50 mm i.d. near-horizontal acrylic pipe. The experimental parameters are the injected water velocity, the height of the initial water layer in the pipe and the pipe inclination.

2. DESCRIPTION OF THE PHENOMENON

Figure 1 shows a schematic diagram of the phenomenon that has been studied. A liquid front advances with velocity V_t over a liquid layer moving at a lower velocity V_f. The layer is overtaken

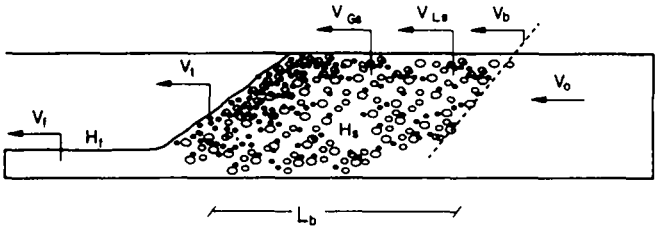

Figure 1. Schematic diagram of the phenomenon. The liquid front advances over a liquid film and gas is entrained into the liquid body.

by the advancing front and accelerated to the mean liquid velocity in the slug, V_{Ls}. In a mixing zone at the front of the slug, a strong swirl is present with a high degree of aeration. Experimental observations show that above a minimum relative velocity between the two liquid streams, air is released from the mixing zone and penetrates into the liquid body. Behind the advancing front, a region of approximately constant gas volume fraction ϵ_s (void fraction) is formed. The length of the aerated region, L_b, increases as the front moves downstream.

The gas volumetric flux per unit pipe area entering the liquid front, Q, equals the total rate of change of the gas content in the slug. Neglecting gas density changes, this may be written as

$$Q = \frac{d}{dt}\int_0^{L_b} \epsilon \, dx, \qquad [1]$$

where ϵ is the cross-sectional void fraction and L_b is the length of the aerated region.

The space-averaged void fraction in the bubble region may be defined as

$$\epsilon_s = \frac{1}{L_b}\int_0^{L_b} \epsilon \, dx. \qquad [2]$$

This gives

$$Q = \frac{d}{dt}(\epsilon_s L_b). \qquad [3]$$

If ϵ_s is constant in time, the gas volume balance relative to the front becomes

$$Q = \epsilon_s(V_t - V_b), \qquad [4]$$

as

$$\frac{dL_b}{dt} = V_t - V_b; \qquad [5]$$

V_t and V_b are the translational velocities of the advancing liquid front and of the border of the bubble region. In [4] and [5] any effect of axial dispersion of bubbles has been neglected.

For constant ϵ_s the volume balances for the gas and the liquid phases with respect to an observer moving at velocity V_b are

$$\epsilon_s(V_{Gs} - V_b) = 0 \qquad [6]$$

and

$$(1 - \epsilon_s)(V_{Ls} - V_b) = (V_0 - V_b), \qquad [7]$$

where V_{Gs} is the gas velocity in the aerated slug and V_0 is the velocity in the bubble-free region. The sum of [6] and [7] gives

$$\epsilon_s V_{Gs} + (1 - \epsilon_s)V_{Ls} = V_0. \qquad [8]$$

Equation [8] represents the conservation of volumetric flow rate across the border of the bubbly region.

From [6] it is seen that the gas velocity in the slug (V_{Gs}) is equal to the velocity of the dispersed bubble front (V_b). The liquid velocity in the aerated slug (V_{Ls}) is related to the film flow rate (V_f) by a liquid volume balance with respect to an observer moving at V_t:

$$(V_t - V_f)H_f = (V_t - V_{Ls})H_s, \quad [9]$$

where H_f and H_s are the liquid volume fractions (holdup) in the film and in the slug, respectively.

The gas entrainment rate may be determined experimentally from [1] or from [4]. For this purpose the spatial integral in [1] must be transformed into a time integral since the available experimental measurements are time traces of liquid volume fractions at given locations in the pipe. This may be done under the abovementioned assumption that the gas phase in the slug moves with constant average velocity V_b. Using [1] at two measuring stations we obtain:

$$Q = \frac{V_b}{\Delta T}\left(\int_0^\infty \epsilon_2 \, dt - \int_0^\infty \epsilon_1 \, dt\right), \quad [10]$$

where ΔT is the transit time of the front between the measuring stations and ϵ_i is the void fraction in the liquid body at station i.

If the mean void fraction ϵ_s in [4] is well-defined and constant in time Q can be determined directly since all quantities in [4] can be measured.

The pressure drop required to accelerate the liquid film to the velocity in the liquid body (Δp_a) is given from an integral liquid momentum balance between the film region and the slug region:

$$\Delta p_a = \rho_L[H_f(V_f - V_t)^2 - H_s(V_{Ls} - V_t)^2], \quad [11]$$

where ρ_L is the liquid density.

Elimination of H_s by [9] gives (Dukler & Hubbard 1975):

$$\Delta p_a = \rho_L[H_f(V_f - V_t)(V_f - V_{Ls})]. \quad [12]$$

3. EXPERIMENTS AND DATA ANALYSIS

The experiments described in the present work consisted of the sudden injection of pure water in a slightly inclined pipe in which a liquid film was flowing downwardly in steady motion. The experiments were conducted at atmospheric conditions in a near-horizontal 17 m long test section of 49.7 mm i.d. Plexiglas pipe. The experimental set-up is shown schematically in figure 2 and has been described by Andreussi & Bendiksen (1989).

The time-varying liquid holdup in the pipe was measured at three fixed locations by means of conductance ring probes. The method has been described and tested for the stratified and bubble phase configuration by Andreussi *et al.* (1988). The measuring stations were positioned

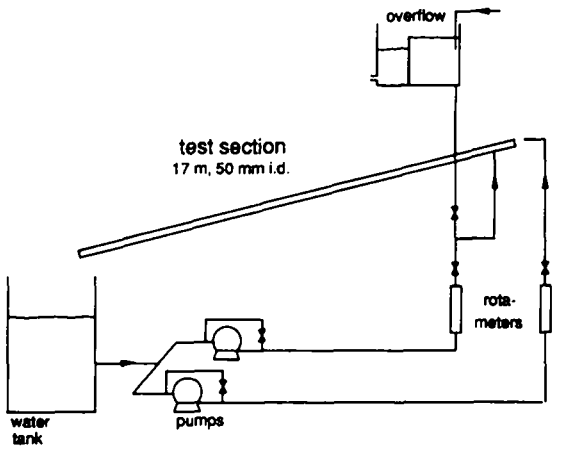

Figure 2. Schematic diagram of the experimental set-up.

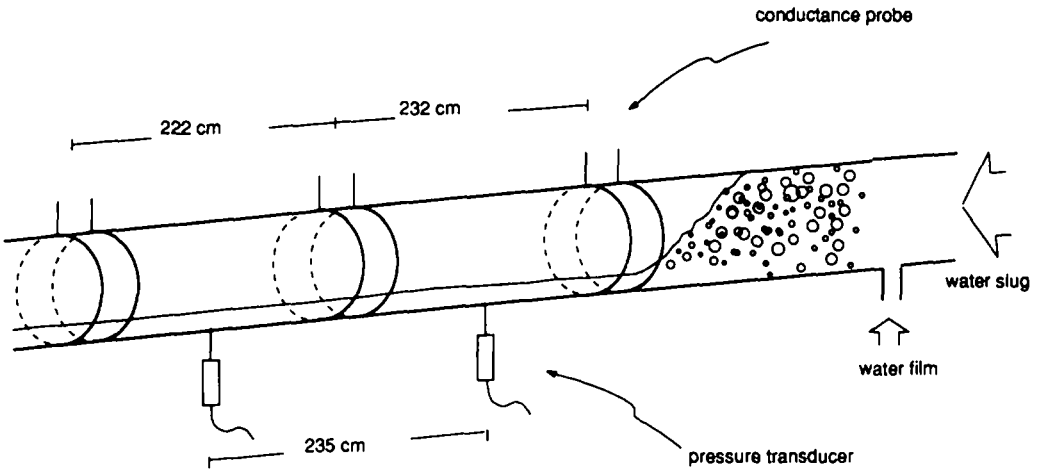

Figure 3. The positioning of the conductance ring probes and the pressure transducers.

approximately at the middle of the pipe. Figure 3 shows the position of the conductance probes together with the position of two piezo-resistive absolute pressure transducers. The pressure transducers were carefully calibrated and the measured single-phase liquid pressure drop agreed to within 10% with smooth pipe predictions.

The flow rate of the injected water was measured with a calibrated rotameter. The measured velocity of an advancing water front in an empty pipe confirmed the calibration within a maximum discrepancy of 3%. Due to the increasing head on the pump the water velocity decreased somewhat as the front moved down the pipe. This decrease was generally $< 5\%$. The reproducibility (standard deviation from the mean value) of the velocities V_t and V_b was within 2%.

Tap water for the film flow was fed to the pipe with a small pump or from a water tank with a constant water level. The flow rate was measured with a calibrated rotameter. Very small flow rates at the lowest pipe inclination were determined directly by measuring the volume of water flowing out of the pipe in a given time interval.

The height of the liquid film was controlled by varying the inclination of the pipe (0–3°) and the input flow rate. The measured holdup in the film generally agreed within 5% with predictions based on the equations given by Andreussi & Persen (1987).

Data acquisition on the computer (3 kHz sampling rate) was triggered by the signal from a capacitance probe mounted on the outside of the pipe.

The experimental procedure was as follows:

- Film flow rate and pipe inclination were adjusted to obtain the desired film holdup.
- The position of the capacitance trigger was determined and the computer activated.
- The film flow was closed at the same time as the large water front was released into the pipe by the sudden opening of a valve. The flow rate was observed on the rotameter during the run.
- Three to six runs were performed for each experimental condition.

Four experimental series were performed. Two series at pipe inclinations close to the horizontal; in one of the two the film was almost stagnant. One series at 3° upwards and one at 3° downwards flow. In each series the film height and the injected velocity of the water front were varied.

A typical output of an experimental run is shown in figure 4. The signals from the conductance probes have been converted to holdup and the pressure is relative to the initial value corresponding to steady film flow conditions. The three holdup signals show the arrival of the water front and the growth of the bubble region in the liquid body moving down the pipe. The initial rise in the two pressure signals gives the pressure drop due to the acceleration of the film to the liquid velocity in the slug.

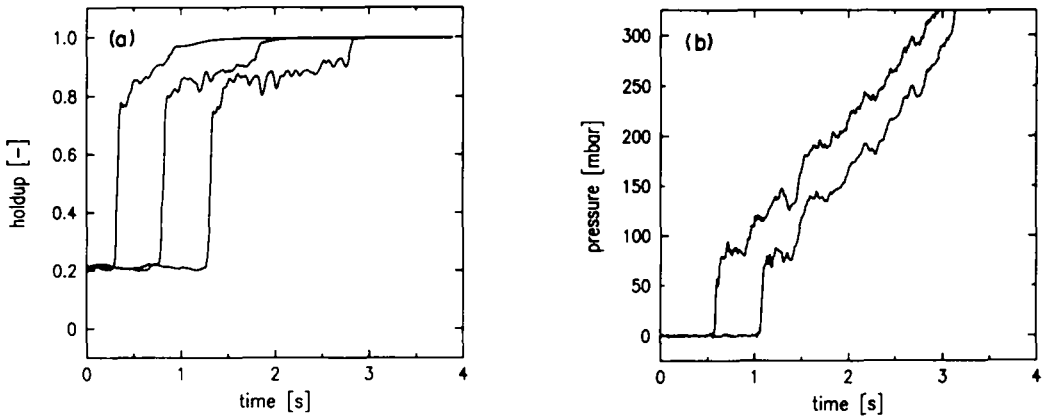

Figure 4. Example of holdup (a) and pressure signals (b). $H_f = 0.21$, $V_0 = 2.7$ m/s and pipe inclination upwards $\theta = 2.7°$.

Figure 5 shows the same experiment performed without an initial water level in the pipe. What can be observed from this example is general: without a film in the pipe the pressure increases monotonically without any initial jump and negligible gas is entrained into the bulk of the slug.

From the holdup and pressure time traces the following parameters have been determined:

- water front velocity, V_l;
- bubble border velocity, V_b;
- accelerational pressure drop, Δp_a;
- mean void fraction in the liquid body, ϵ_s;
- holdup in the liquid film, H_f.

The analysis is performed with the aid of graphical software.

The velocities have been determined from the time interval that gave the best overlap of the ramps in the holdup time traces. The definition of the ramps due to the arrival of the slug front and of the border of the dispersed bubble region was done by positioning graphical markers on the computer screen.

The mean gas void fraction was computed from the central flat region of the signal which was defined with graphical markers.

The gas bubble production rate has been obtained using both [4] and [10], the agreement was generally in the order of the spread of the results relative to the same experimental conditions. The reported values are those obtained by [10], which was considered to be the more precise method.

The magnitude of the initial rise in the pressure signals (Δp_a) was determined with graphical markers.

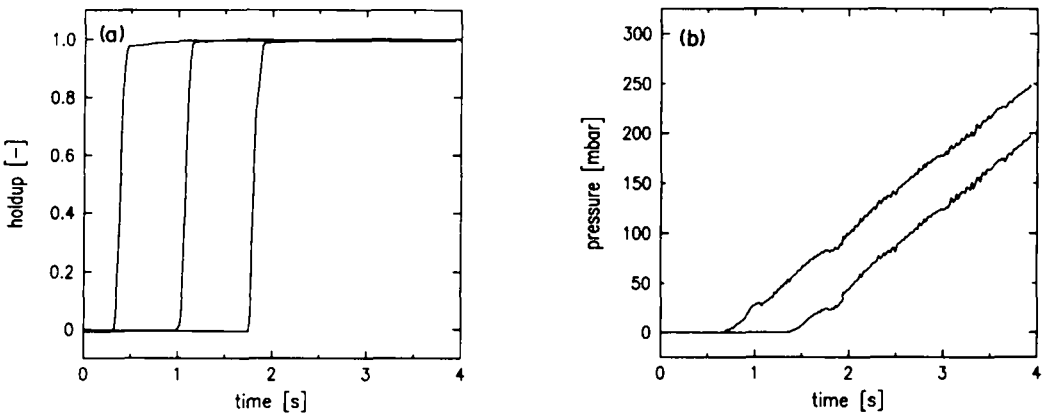

Figure 5. Example of holdup (a) and pressure signals (b) with no initial liquid film in the pipe. $V_0 = 2.7$ m/s and pipe inclination upwards $\theta = 2.7°$.

The velocities and the bubble production rates were determined between the two first and the two last conductance probes. The final values reported are the mean values of the two. In a few high velocity cases the flow was clearly more developed between the two final probes than between the first two, in the sense that a constant holdup level was not observed at the first station. In these cases only data obtained from the last two probes are reported.

Table 1. Experimental results

V_t (m/s)	V_b (m/s)	V_0 (m/s)	Δp_a (mbar)	θ (deg)	Q (m/s)	H_s (—)	H_f (—)	V_{sf} (m/s)
3.00	2.15	2.65	13.33	−0.36	0.025	0.964	0.126	0.028
3.70	2.59	3.36	15.94	−0.36	0.036	0.972	0.096	0.028
4.54	3.36	4.09	23.10	−0.36	0.060	0.948	0.097	0.028
5.22	4.10	4.66	35.28	−0.36	0.099	0.918	0.096	0.028
7.27	6.35	5.79	55.68	−0.36	0.176	0.845	0.094	0.028
3.00	1.89	2.62	10.73	−0.16	0.030	0.964	0.172	0.029
3.89	2.52	3.34	17.97	−0.16	0.067	0.952	0.172	0.029
4.82	3.16	4.07	30.64	−0.16	0.110	0.930	0.175	0.029
5.74	4.10	4.74	42.38	−0.16	0.170	0.901	0.176	0.029
7.92	6.22	5.84	62.99	−0.16	0.300	0.871	0.175	0.029
3.44	1.92	2.66	22.59	−0.12	0.066	0.969	0.276	0.046
4.45	2.57	3.36	32.49	−0.12	0.114	0.935	0.276	0.046
5.32	3.15	3.98	45.40	−0.12	0.183	0.922	0.275	0.046
6.44	4.11	4.73	62.60	−0.12	0.248	0.898	0.275	0.046
8.79	6.33	5.99	125.67	−0.12	0.428	0.838	0.269	0.046
3.00	2.83	2.68	15.17	−0.42	0.013	0.880	0.114	0.035
3.79	2.57	3.40	21.90	−0.42	0.054	0.964	0.112	0.032
4.45	3.13	4.02	23.85	−0.42	0.069	0.918	0.122	0.030
5.33	3.97	4.73	34.58	−0.42	0.122	0.907	0.124	0.033
6.13	3.65	4.66	58.03	−0.42	0.247	0.887	0.224	0.086
5.17	3.02	4.05	42.15	−0.42	0.164	0.912	0.226	0.087
4.44	2.52	3.47	28.27	−0.42	0.121	0.929	0.227	0.088
3.35	1.94	2.65	18.00	−0.42	0.059	0.949	0.225	0.083
4.05	2.04	2.71	28.98	−0.42	0.132	0.932	0.320	0.143
5.13	2.51	3.41	43.76	−0.42	0.206	0.918	0.321	0.143
5.96	2.94	4.01	63.12	−0.42	0.246	0.911	0.320	0.143
7.24	3.64	4.77	95.04	−0.42	0.381	0.885	0.322	0.143
2.23	1.79	1.95	12.85	2.72	0.042	0.923	0.102	0.090
3.16	2.17	2.72	19.56	2.72	0.092	0.895	0.104	−0.090
3.15	2.19	2.79	19.19	2.72	0.091	0.900	0.105	−0.090
3.97	2.69	3.39	31.78	2.72	0.142	0.885	0.114	−0.090
4.57	3.15	3.94	38.69	2,72	0.150	0.887	0.101	−0.090
5.40	4.34	4.73	49.34	2.72	0.169	0.885	0.089	−0.090
6.55	5.58	5.73	78.30	2.72	0.254	0.853	0.106	−0.090
1.93	1.17	1.24	21.95	2.72	0.078	0.970	0.212	−0.244
2.91	1.69	1.95	32.18	2.72	0.137	0.947	0.211	−0.244
3.90	1.97	2.69	49.54	2.72	0.207	0.897	0.210	−0.244
4.86	2.52	3.34	71.78	2.72	0.279	0.872	0.213	−0.244
5.64	3.11	3.94	90.80	2.72	0.322	0.864	0.213	−0.244
6.59	4.03	4.66	110.92	2.72	0.342	0.860	0.206	−0.244
7.57	5.21	5.62	163.99	2.72	0.461	0.817	0.207	−0.244
3.68	2.34	1.95	57.65	2.72	0.251	0.861	0.302	−0.416
4.93	2.02	2.79	82.64	2.72	0.322	0.889	0.301	−0.416
5.84	2.51	3.34	120.76	2.72	0.408	0.893	0.300	−0.416
6.70	3.15	3.94	152.40	2.72	0.452	0.884	0.299	−0.416
7.36	4.04	4.53	194.47	2.72	0.465	0.860	0.302	−0.416
8.48	5.04	5.56	281.84	2.72	0.551	0.860	0.300	−0.416
3.76	3.53	3.34	15.96	−3.02	0.010	0.968	0.077	0.053
4.28	3.71	3.98	14.18	−3.02	0.035	0.950	0.079	0.053
4.95	4.14	4.60	28.96	−3.02	0.049	0.913	0.077	0.053
5.78	4.50	5.02	36.99	−3.02	0.127	0.888	0.135	0.109
4.46	3.16	3.94	24.12	−3.02	0.066	0.946	0.129	0.109
3.73	2.87	3.27	15.78	−3.02	0.023	0.951	0.130	0.109
4.21	2.63	3.32	19.35	−3.02	0.066	0.951	0.204	0.200
5.07	3.30	4.07	35.84	−3.02	0.104	0.926	0.204	0.200
6.01	4.12	4.79	52.54	−3.02	0.178	0.897	0.202	0.200
7.08	4.43	4.73	78.92	−3.02	0.271	0.891	0.292	0.360
5.89	3.50	4.02	52.50	−3.02	0.200	0.914	0.289	0.360
4.90	2.81	3.56	33.57	−3.02	0.125	0.938	0.291	0.360
3.85	2.51	2.88	15.96	−3.02	0.038	0.967	0.300	0.360

Each point in the table represents the mean value of 3–6 experiments.

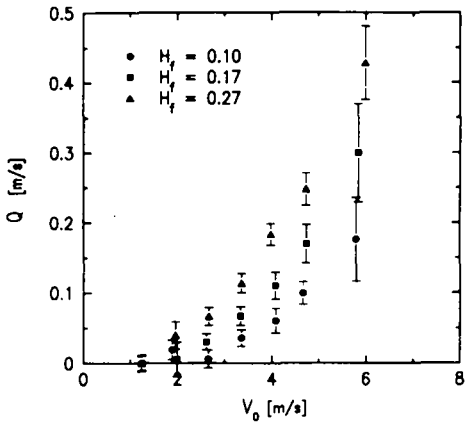

Figure 6. Gas entrainment rate (Q) vs inlet liquid velocity (V_0) for three film volume fractions (H_f). The pipe inclination is close to horizontal ($\theta < 0.4°$). Q is the volumetric gas flux per unit pipe area that enters the advancing liquid front.

4. RESULTS AND DISCUSSION

The experimental results are reported in table 1. Each point in this table represents the mean value of 3–6 experiments.

One series of measurements of the gas entrainment volumetric flux (Q) is plotted in figure 6 vs the liquid velocity (V_0). The error bars represent the standard deviation from the mean value. As can be seen from this figure, the gas entrainment rate increases with increasing film holdup and increasing liquid velocity.

The gas entrainment rate can be assumed to be a function of the film holdup ahead of the front, the relative velocity between the film and the slug, the pipe geometry, the fluid properties and the pressure. In these experiments only the holdup and velocities are varied, therefore a gas entrainment relation is sought in terms of these parameters.

The data indicate that the entrainment rate to a first approximation is a linear function of the relative velocity between the film and the liquid front. This may be written as

$$Q = c_1[(V_t - V_f) - c_2], \qquad [13]$$

where the coefficients c_1 and c_2 are functions of the film holdup.

The results obtained from a linear regression on all data sets are shown in figure 7, where c_1 and c_2 are plotted vs the non-dimensional interfacial width (S_i/d). The error bars are uncertainty estimates based on regression analysis results with the exclusion of end points. The slope factor

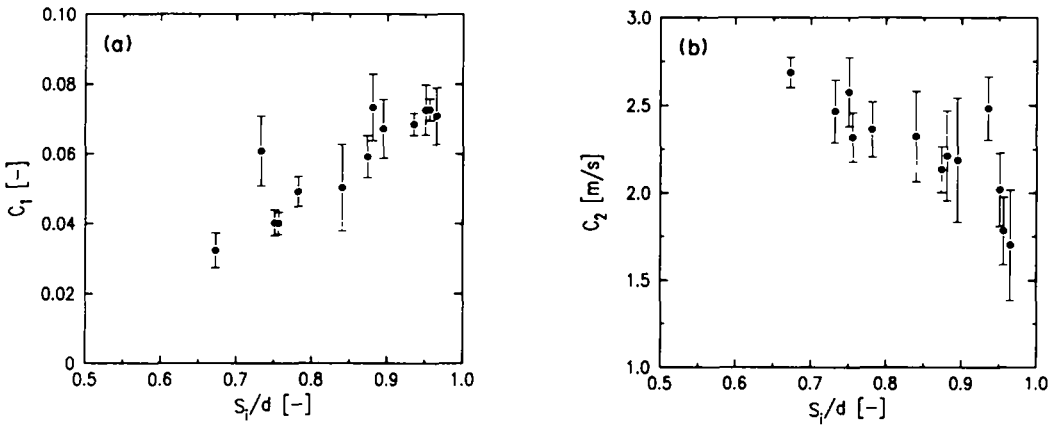

Figure 7. Results from linear regression analysis of the data to [13]. The coefficients c_1 (a) and c_2 (b) are plotted vs the non-dimensional interfacial width (S_i/d). The error bars are uncertainty estimates based on regression analysis results with the exclusion of end points.

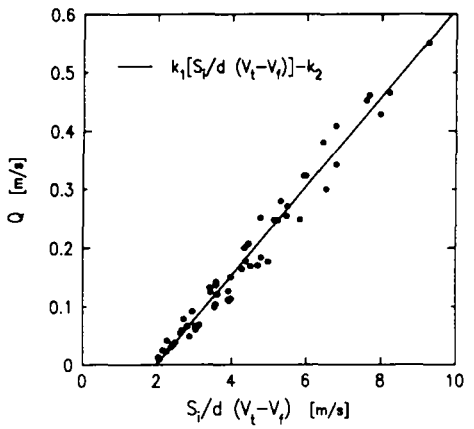

Figure 8. Experimental gas entrainment data (Q) compared with [14]. $k_1 = 0.076$ and $k_2 = 0.15$ m/s.

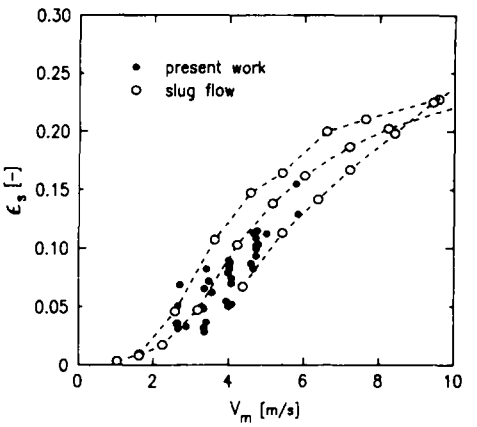

Figure 9. Mean gas volume fraction in the slug (ϵ_s) vs mixture superficial velocity (V_m). The single points are the present results for a near-horizontal pipe, $V_m = V_0$. The connected points are the void fraction in the slugs in horizontal slug flow, $V_m = V_{Ls} + V_{Gs}$. The three curves are for three liquid superficial velocities, $V_{Ls} = 0.6$, 1.2 and 2.4 m/s, where a high void fraction corresponds to a low liquid velocity.

c_1 increases and the onset for entrainment c_2 decreases with the interfacial width S_i. The product $c_2 S_i$ is fairly constant, so that the final expression for Q may be given as

$$Q = k_1 \frac{S_i}{d} (V_t - V_f) - k_2. \qquad [14]$$

This equation is compared with measurements in figure 8. Linear regression analysis gives the coefficient values:

$$k_1 = 0.076 \quad \text{and} \quad k_2 = 0.15 \text{ m/s}.$$

Equation [14] is in good agreement with the expression for the total air entrainment into a slug suggested by Andreussi & Bendiksen (1989), except that S_i/d is used instead of H_f since this gave a better fit to the data.

As can be seen from [13] and [14] and in figure 8, the entrainment rate is zero for

$$V_t - V_f = \frac{k_2}{k_1 \frac{S_i}{d}} \qquad [15]$$

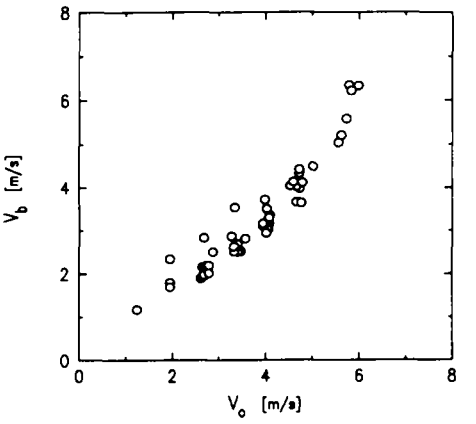

Figure 10. Velocity of the dispersed bubble border (V_b) vs the inlet liquid velocity (V_0).

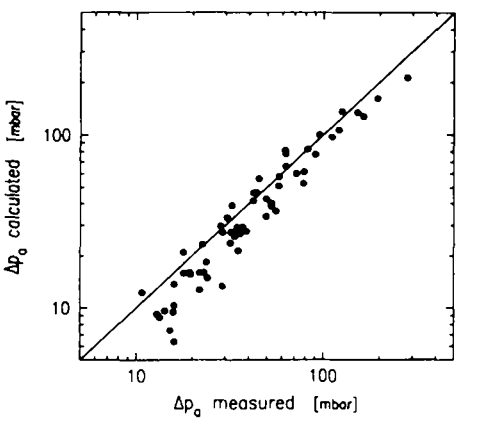

Figure 11. Measured pressure drop due to the acceleration of the liquid in the film to the velocity in the slug compared with calculated values by [12].

This result seems to correspond with similar observations reported by Kalinske & Robertson (1943), among others, and with the measurements of void fraction in slugs recently presented by Andreussi & Bendiksen (1989), in which $\varepsilon_s = 0$ below a limiting value of the velocity difference $V_t - V_f$.

To compare the present experiments with slug flow at similar conditions the void fractions in slugs were measured for horizontal slug flow. The data for the mean void fraction in the bubbly region are plotted in figure 9 together with data obtained for the void in the slugs under slug flow conditions. The present void fraction values are plotted vs the water velocity (V_0) which, according to [8], is equal to the mixture velocity in the bubbly region (V_m). The data for the void in the slugs have been obtained in the same pipe with liquid superficial velocities equal to 0.6, 1.2 and 2.4 m/s and gas superficial velocities (at standard conditions) up to 10 m/s. Each point represents the mean value of the void fraction in more than a hundred slugs. The data are plotted vs the mixture velocity $V_m = V_{Ls} + V_{Gs}$ which is approximately equal to the gas and liquid velocity in the slugs. The data from the two experiments compare well, indicating that the present experiment is similar to the more complex case of slug flow in a pipe.

The velocity of the border to the bubble-free region (V_b) is plotted vs the liquid velocity (V_0) in figure 10. At low void fraction $V_b < V_0$, but it increases to approximately the same value as the void fraction and the velocity increase. The general observation that the shape of the bubble border ramp in the holdup time traces is the same between measuring stations justifies the assumption that the dispersed bubbles move with the same velocity as the bubble border, or that axial dispersion effects are negligible.

The velocities V_b are smaller than those reported for vertical dispersed bubble flow (Wallis 1969; Mishima & Ishii 1984), where the slip ratio has been found to be equal to or larger than one.

To the authors knowledge no data on slip in horizontal bubble flow are available in the literature. The appreciable slip indicated by the present data may probably not be explained in terms of a variation of slip over the pipe cross section, caused by the large bubble concentration close to the top (due to buoyancy). Other complex effects may be important for appreciable bubble concentrations and detailed experiments are underway at the University of Pisa in order to determine local bubble concentration and velocity under conditions of fully-developed bubble flow. Preliminary results have been reported by Andreussi *et al.* (1990).

The measured acceleration pressure drops are compared with [12] in figure 11. The liquid velocity in the bubbly region (V_{Ls}) is determined by [7]. V_{Ls} can also be determined from [9]. The values determined by these two methods agree within 10%. The agreement between the computed and the measured accelerational pressure drop is generally within 25%.

Very little work is reported in the literature on gas entrainment in closed conduit flow, most of it concerns entrainment into a stationary liquid level.

Ahmed *et al.* (1985) carried out an extensive experimental study on air entrainment caused by falling film that penetrates into a stationary water front in a rectangular channel. They developed a rather complicated empirical correlation which was also compared with data from similar experiments reported by other workers:

$$Q = K(V_f - 0.8)^3, \qquad [16]$$

where

$$K = K(\mathrm{Fr}, V_c), \qquad [17]$$

Fr is the film Froude number ($\mathrm{Fr} = \sqrt{V_f/gh_f}$), h_f is the film height, V_c is the critical outlet velocity for the onset of gas entrainment and g is the acceleration of gravity.

The phenomenon of a falling film entering a stationary front in a channel is different from the present case with a moving front in a pipe. A few qualitative similarities may, however, be noted. The gas entrainment increases with increasing film velocity relative to the front, although a power of 3 is too strong at high velocities in the present case. The critical relative film velocity for the onset of net gas entrainment decreases with increasing film height. The values are in the same range as in our case: 2–4 m/s. The dependency of the gas entrainment rate on the film height is not clear. The length from the film inlet to the stationary liquid level was reported to affect the gas entrainment rate; a stationary film flow may not have been established at the point of penetration.

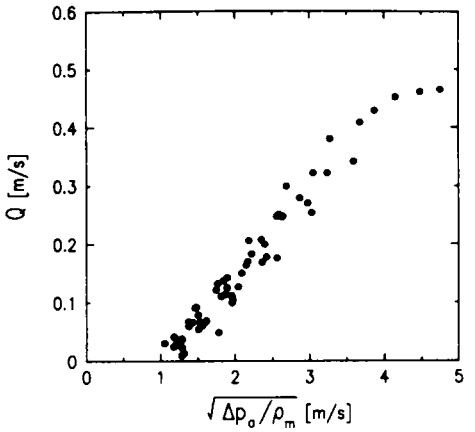

Figure 12. Gas entrainment rate (Q) vs the characteristic velocity $\sqrt{\Delta p_a/\rho_m}$. Q is the volumetric gas flux per unit pipe area entering the liquid front, Δp_a is the pressure drop due to the acceleration of the film.

In the work of Kalinske & Robertson (1943) aeration caused by a falling film entering a stationary hydraulic jump in a pipe was studied in a set-up similar to that of Ahmed *et al.* (1985). No effect of film height and pipe inclination was noted, and the entrainment rate was correlated by the equation

$$\beta = \frac{Q_G}{Q_L} = 0.0066(\mathrm{Fr} - 1)^{1.4}, \qquad [18]$$

where Fr is the film Froude number ($\mathrm{Fr} = V_f/\sqrt{gA_f/S_i}$), Q_G is the gas discharge, Q_L is the liquid discharge and A_f is the film cross-sectional area.

The ratio of the gas to liquid flux into the water front was argued to be a function of Fr because the strong swirl in the front of the jump represents energy loss that can be related to Fr.

Our case of an advancing front is different and the term "hydraulic jump" may be misleading since the term is usually given to free surface flow, where the pressure is given by the static head. In our case, a steep advancing water front may even be sustained in an empty pipe provided that the velocity is high enough. Furthermore, the velocity profiles in the two phenomena and the roughness of the film and the water front are different. The large difference in the liquid velocities in the slug for the two experiments also gives a different turbulence level and therefore different capacity for bubble breakup and dispersion.

Correlation of our data with Fr, as for the gravity controlled hydraulic jump, proved unsuccessful. The insufficiency of Fr as a scaling parameter was demonstrated by Ahmed *et al.* (1985) and more generally noted by Kenn & Zanker (1967). The suggestion that the air entrainment rate should depend on the strength of the swirl at the slug front appears to be more fruitful. The violent eddies at the water front are created by the pressure force necessary to accelerate the film to the water velocity, Δp_a. A characteristic velocity related to this force is

$$\sqrt{\frac{\Delta p_a}{\rho_m}}; \qquad [19]$$

where ρ_m is the mixture density,

$$\rho_m = \rho_G \epsilon_s + \rho_L(1 - \epsilon_s). \qquad [20]$$

As shown in figure 12, our data for air entrainment show a linear correlation with this characteristic velocity.

5. CONCLUSIONS

It has been shown that the rate of gas entrainment into a liquid front advancing over a liquid film in a pipe can be determined from measurements of the gas content in the liquid body at various locations.

The experimental results show that:

1. Gas entrainment only occurs if a liquid layer is present ahead of the advancing slug. Moreover, the relative velocity between the moving front and the liquid layer must be greater than a limiting value.
2. The rate of net gas entrainment is approximately proportional to the relative velocity between the front and the layer, and to the length of the interfacial width of the layer.
3. Measured pressure drops, film heights, gas volume fraction in the advancing slug agree well with available correlations or with similar measurements taken under conditions of fully developed slug flow.

The experimental measurements described in this paper could in a future work be extended to different pipe sizes and fluid properties in order to obtain a more general physical model for the gas entrainment phenomenon.

Acknowledgements—The authors wish to thank Professor K. Bendiksen for discussions and support during the work. We are also grateful to S. Pintus for the design of the data acquisition system.

O. J. Nydal acknowledges the fellowship received by The Norwegian Council for Technical Research (NTNF). The work has been supported by the Commission of the European Communities, under Contract EN3G-0047/I.

REFERENCES

AHMED, A., ERVINE, D. A. & MCKEOGH, E. J. 1985 The process of aeration in closed conduit hydraulic structures. In *Proc. IAHR Symp. on Scale Effects in Modelling Hydraulic Structures*, Session 4, Paper 3, pp. 4.13-1–4.13-7.

ANDREUSSI, P. & BENDIKSEN, K. 1989 An investigation of void fraction in liquid slugs for horizontal and inclined gas–liquid pipe flow. *Int. J. Multiphase Flow* **15,** 937–947.

ANDREUSSI, P. & PERSEN, L. N. 1987 Stratified gas–liquid flow in downwardly inclined pipes. *Int. J. Multiphase Flow* **13,** 565–577.

ANDREUSSI, P., DI DONFRANCESCO, A. & MESSIA, M. 1988 An impedance method for the measurement of liquid hold-up in two-phase flow. *Int. J. Multiphase Flow* **14,** 777–787.

ANDREUSSI, P., PINTUS, S., NYDAL, O., J. & SANCHEZ SILVA, F. A. 1990 Measurements of the mean gas velocity in horizontal and inclined gas–liquid pipe flow. Presented at the *ICHMT Int. Semin. on Phase-interface Phenomena in Multiphase Flow*, Dubrovnik, Yugoslavia.

DUKLER, A. E. & HUBBARD, M. G. 1975 A model for gas–liquid slug flow in horizontal and near horizontal tubes. *Ind. Engng Chem. Fundam.* **14,** 337–347.

KALINSKE, A. A. & ROBERTSON, J. M. 1943 Closed conduit flow. *Trans. ASCE* **108,** 1435–1447.

KENN, M. J. & ZANKER, K. J. 1967 Aspects of similarity for air entraining water flows. *Nature* **213,** 59–60.

MISHIMA, K. & ISHII, M. 1984 Flow regime transition criteria for upward two-phase flow in vertical tubes. *Int. J. Heat Mass Transfer* **27,** 723–738.

WALLIS, G. B. 1969 *One-dimensional Two-phase Flow*, pp. 175–281. McGraw-Hill, New York.